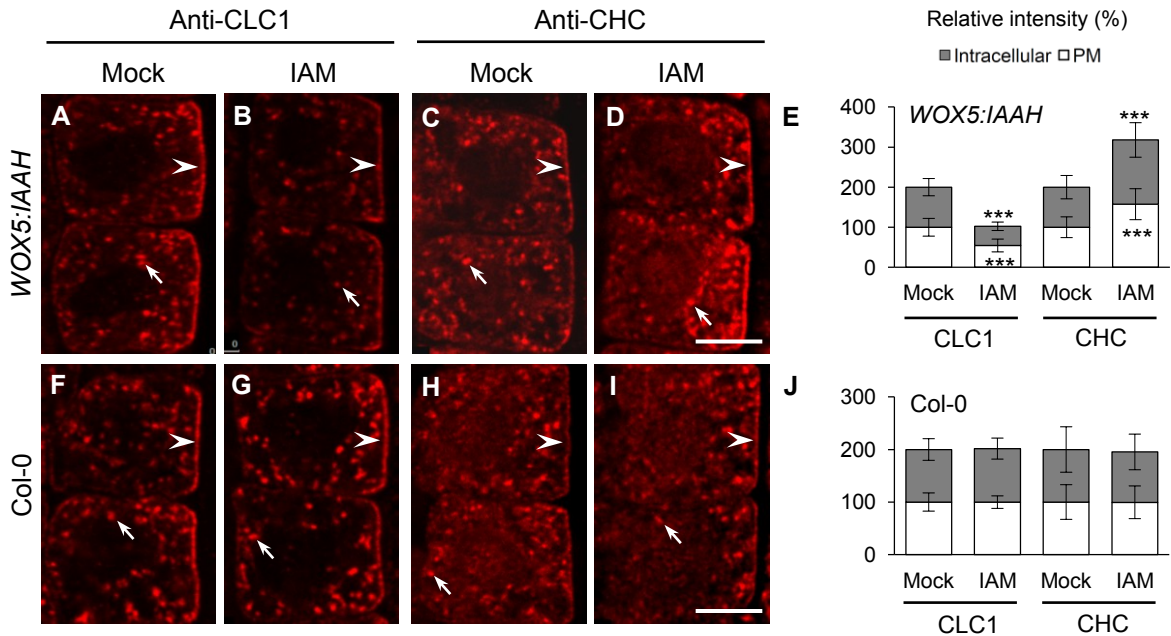


Supplemental Data



Supplemental Figure S1. Elevation of Endogenous Auxin Levels Affects Clathrin Membrane Association.

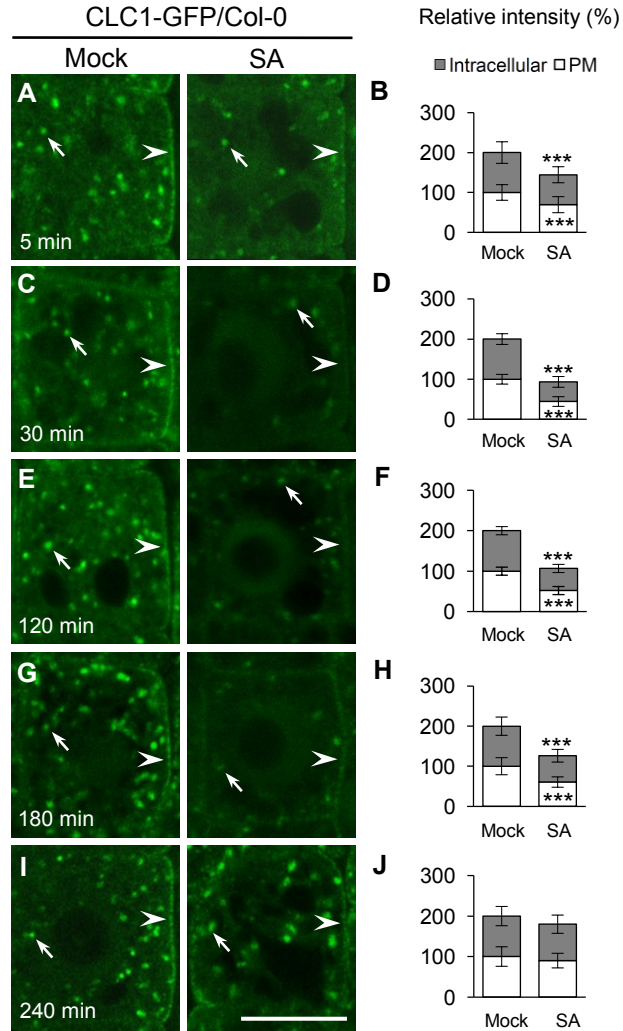
A to E, Differential effects of increased endogenous auxin on the membrane association of CLC1 and CHCs in the *WOX5:IAAH* transgenic lines.

F to J, The effect of IAAH substrate, IAM, on the membrane association of CLC1 and CHCs in the wild-type seedlings.

E and J, The relative intensities of PM- and intracellular compartments-associated CLC1 and CHCs (E, $n = 49-55$ cells from 8 or 9 roots each; J, $n = 39-57$ cells from 7-9 roots each).

Five-day-old vertical grown seedlings were incubated for 90 min in $0.5\times$ MS liquid medium supplemented with mock (DMSO) and IAM ($5\ \mu\text{M}$), respectively, before IF analysis.

Arrows and arrowheads show intracellular compartments- and PM-associated CLC1 or CHCs, respectively. Shown are means \pm SD. Triple asterisks $P < 0.0001$ (Student's t test; compared to the corresponding mock). Scale bars = $7.5\ \mu\text{m}$.

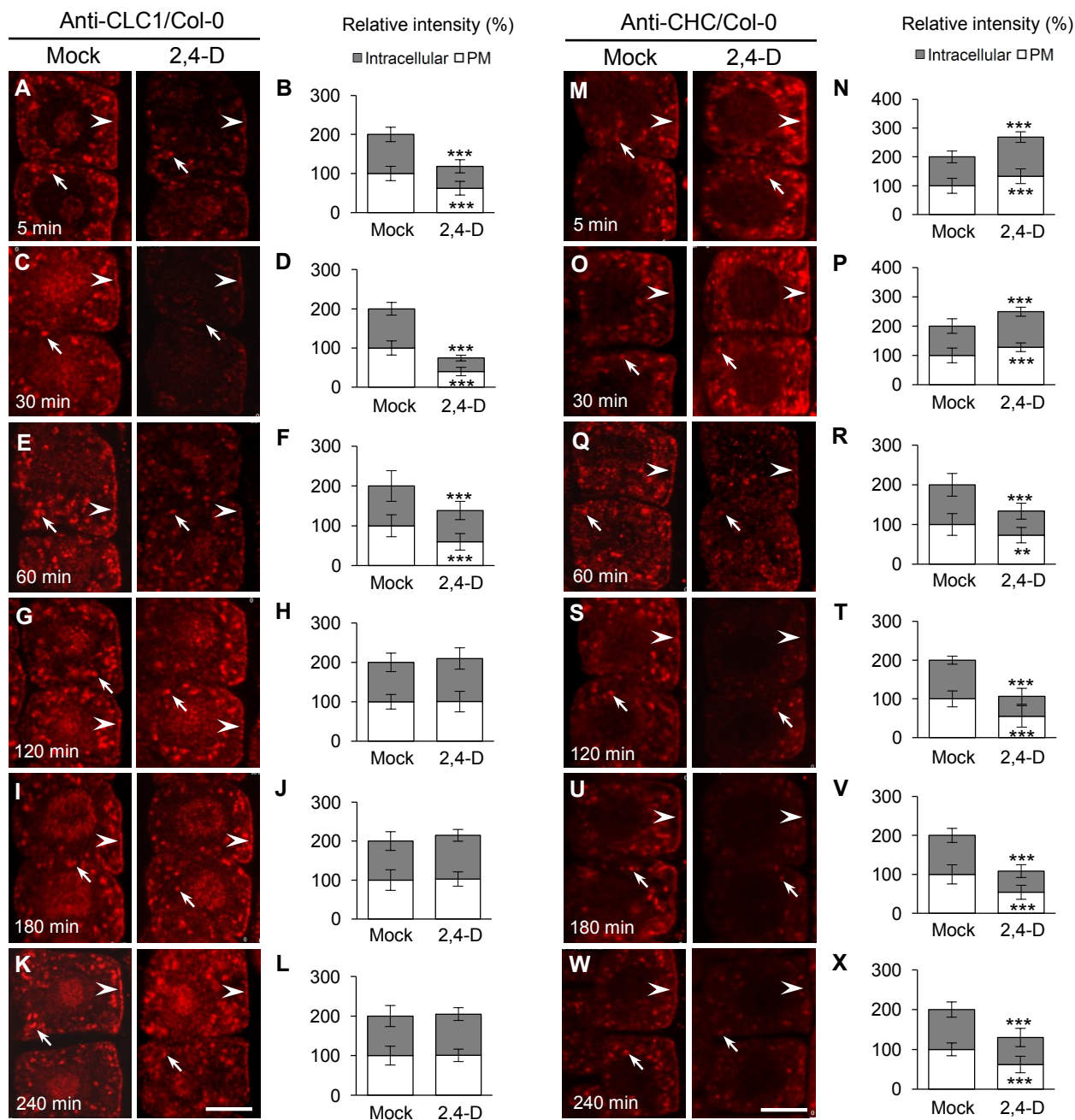


Supplemental Figure S2. Time-Course Analyses of SA Effect on CLC1-GFP Membrane Association.

A to J, The wild-type seedlings expressing CLC1-GFP were treated with mock (DMSO) and SA (25 μ M) for different time lengths, respectively.

B, D, F, H, and J, The relative intensity of CLC1-GFP at the PM and intracellular compartments ($n = 50-65$ cells from 8 roots each).

Different time lengths (5, 30, 120, 180, and 240 min) in mock (DMSO) and SA (25 μ M) treatments are indicated in the lower-left corners of each panel. Arrows and arrowheads show intracellular compartments- and PM-associated CLC1-GFP, respectively. Shown are means \pm SD. Triple asterisks $P < 0.0001$ (Student's t test). Scale bars = 10 μ m.



Supplemental Figure S3. Kinetic Effects of Auxin on the Membrane Association of Clathrin.

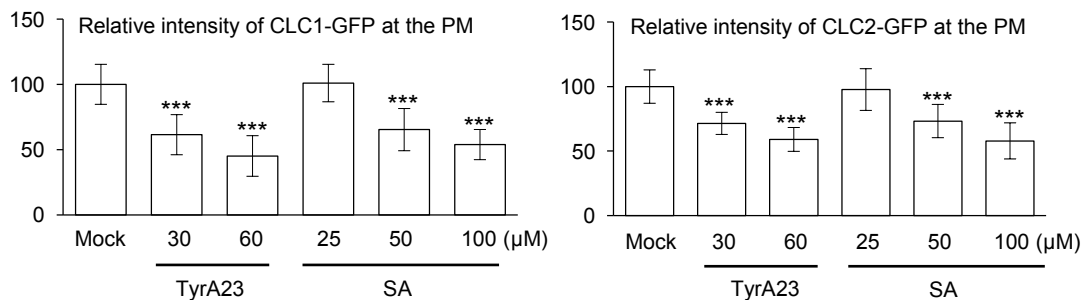
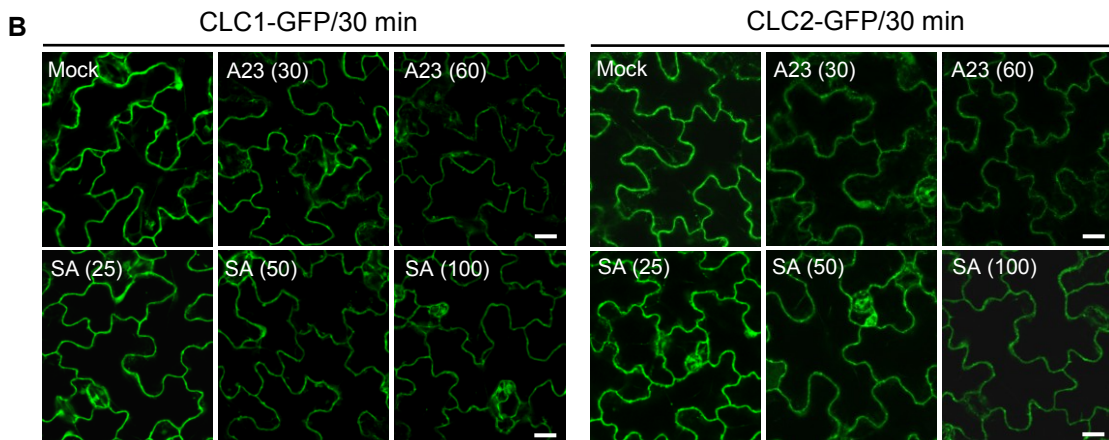
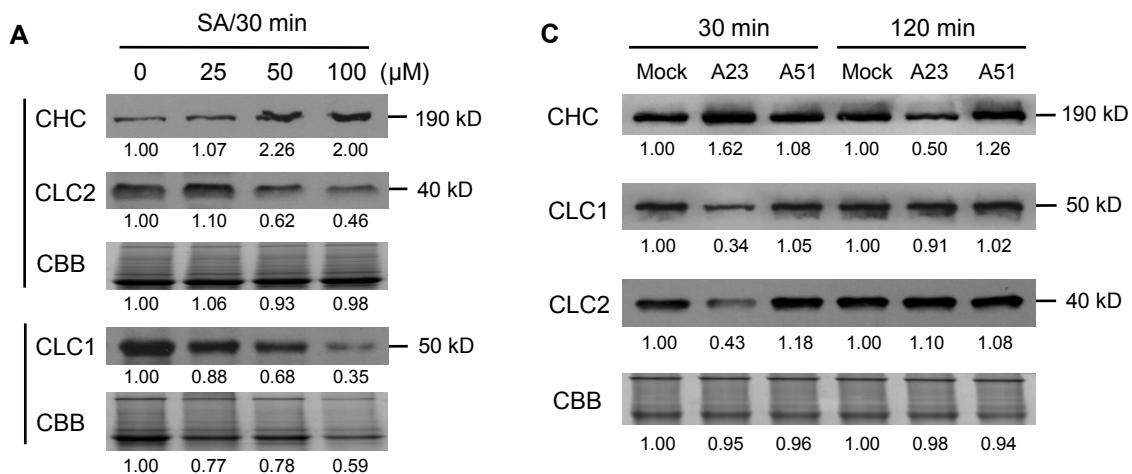
A to L, Auxin effect on PM- and intracellular compartments-associated CLC1 in the wild type.

M to X, Auxin effect on PM- and intracellular compartments-associated CHC in the wild type.

B, D, F, H, J, and L, The relative intensity of CLC1 at the PM and intracellular compartments ($n = 54-90$ cells from 4-6 roots each).

N, P, R, T, V, and X, The relative intensity of CHC at the PM and intracellular compartments ($n = 40-68$ cells from 6-8 roots each).

Different time lengths (5, 30, 60, 120, 180, and 240 min) in mock (DMSO) and 2,4-D (10 μ M) treatments are indicated in the lower-left corners of each panel. Arrows and arrowheads show intracellular compartments- and PM-associated CLC1 or CHC, respectively. Shown are means \pm SD. Double and triple asterisks $P < 0.001$ and 0.0001 , respectively (Student's t test). Scale bars = 10 μ m.

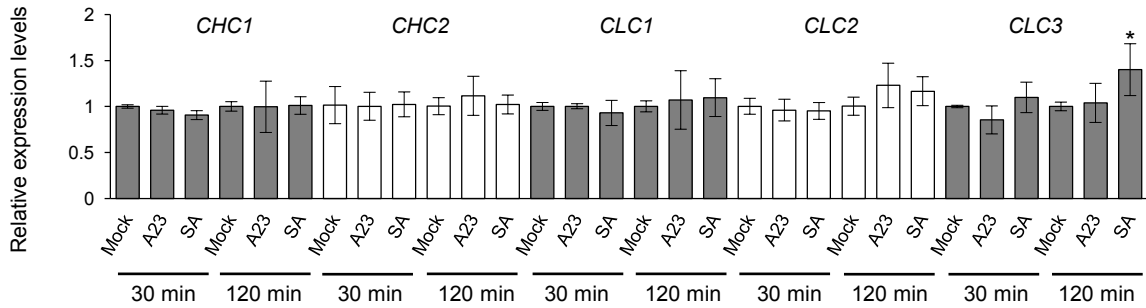


Supplemental Figure S4. Immunoblot and Live-Cell Imaging Analyses of Clathrin Membrane Association.

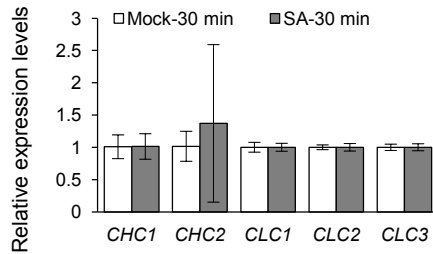
A and C, Immunoblot analysis of the effects of SA (A) and TyrA23 (C) on the membrane association of CLC1/2 and CHC. Five-day-old seedlings grown in 0.5× MS liquid medium under constant light were treated with different SA concentrations (0, 25, 50, and 100 μM) for 30 min (A), TyrA23 (A23; 0 and 30 μM), and TyrA51 (A51; 0 and 30 μM) for 30 min and 120 min (C), respectively. The microsomal membrane fractions were extracted from the whole seedlings. CBB is Coomassie Brilliant Blue R250 and used as a total protein loading control. Numbers at the bottom of each panel indicate band intensities of CHC and CLC1/2 relative to CBB loading controls, normalized to mock controls (1.00). Loading controls were also normalized to their mock controls.

B, Live-cell microscopy analysis of the effects of TyrA23 and SA on CLC1/2-GFP membrane association in the wild-type cotyledon epidermal cells. The numbers in the brackets show SA and TyrA23 concentrations (μM), while treatment time (30 min) is indicated at the top of the panel. The bottom graphs are quantitative data ($n = 77-116$ cells from 18 seedlings each). Shown are means ± SD. Triple asterisks $P < 0.0001$ (Student's t test; compared to the mock control). Bars = 20 μm.

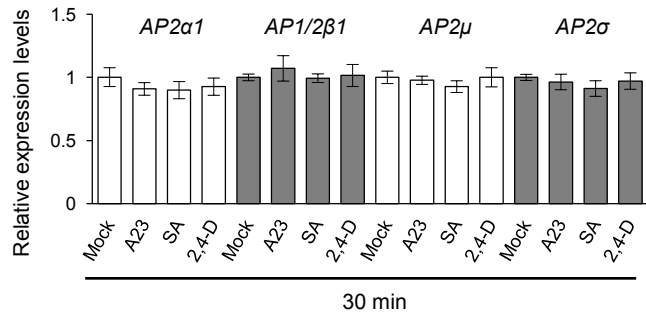
A Col-0 seedlings



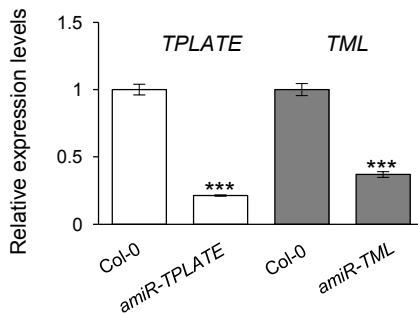
B Col-0 roots



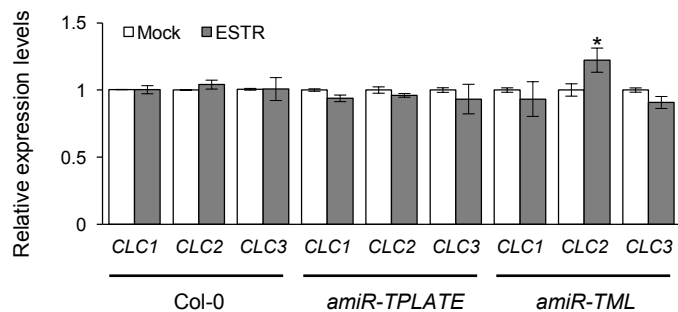
C Col-0 seedlings



D ESTR induction (24 h)



E ESTR induction (24 h)



Supplemental Figure S5. qRT-PCR Analysis of Transcriptional Levels of Clathrin and the AP-2/TPC Subunits.

A, Effects of TyrA23 and SA on the transcriptional levels of *CHC1/2* and *CLC1-3* in whole seedlings.

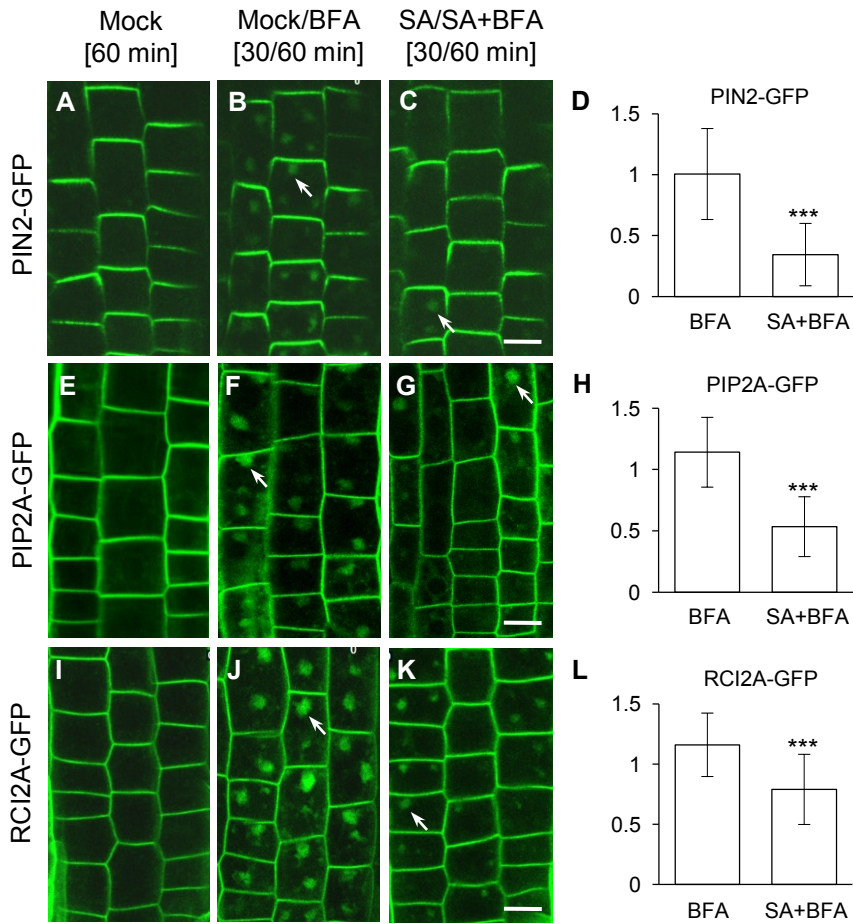
B, SA effect on the transcriptional levels of *CHC1/2* and *CLC1-3* in roots.

C, Effects of TyrA23, SA, and 2,4-D on the transcriptional levels of AP-2 subunits in whole seedlings.

D, Down-regulation of *TPLATE* and *TML* in ESTR-treated *amiR-TPLATE* and *amiR-TML* whole seedlings.

E, Effects of down-regulation of *TPLATE* and *TML* on the transcriptional levels of *CLC1-3* in whole seedlings.

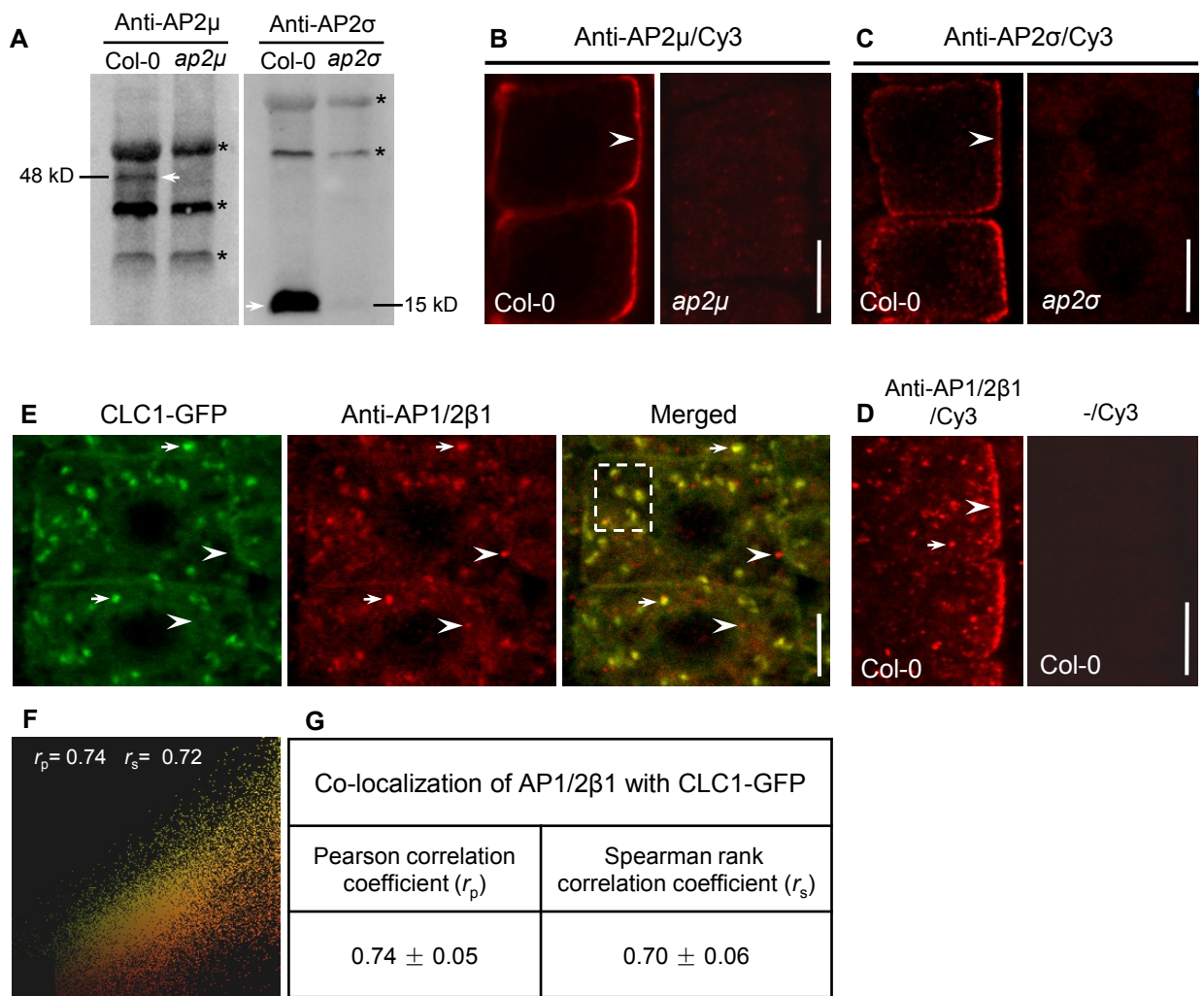
Five-day-old wild-type (Col-0) seedlings (A to C) were treated with mock (DMSO), SA (25 μM), and/or TyrA23 (A23; 30 μM), and/or 2,4-D (10 μM) for 30 min and/or 120 min, respectively, while 4-day-old seedlings (D and E) were treated with ESTR (5 μM) for 24 h. For each gene, the transcription levels in the treatments were presented as a percentage of the corresponding mock or wild-type control. Shown are means ± SD. Single and triple asterisks indicate P < 0.05 and 0.001, respectively (Student's *t* test; compared with the corresponding mock or wild-type control).



Supplemental Figure S6. Effects of Low Concentrations of SA on Internalization of PM Proteins.

A to L, Five-day-old seedlings expressing PIN2-GFP (A to D), PIP2A-GFP (E to H), RC12A-GFP (I to L) were pretreated with mock (DMSO) and SA (25 μ M) for 30 min followed by washout with mock (DMSO), BFA (50 μ M), and SA plus BFA for 60 min, respectively.

D, H, and L, The average number of GFP-labeled BFA bodies ($n = 373$ -522 cells from 14-16 roots each). Arrows show GFP-labeled BFA bodies. Shown are means \pm SD. Triple asterisks $P < 0.0001$ (Student's t test). Scale bars = 10 μ m.



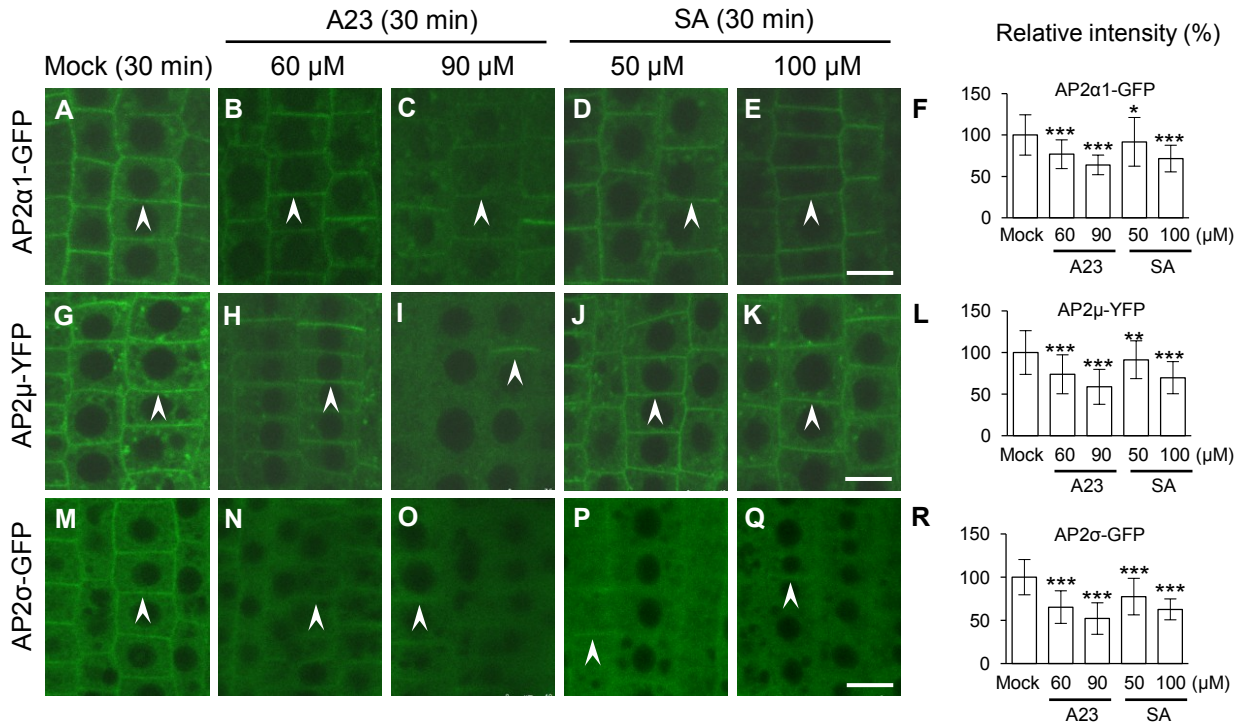
Supplemental Figure S7. Immunoblot and IF Analyses of the AP-2 Antibodies.

A to C, Immunodetection of endogenous AP2 μ and AP2 σ in the wild type, *ap2 μ* , and *ap2 σ* . A, Immunoblot analysis of total protein extracts from leaf tissues using anti-AP2 μ and anti-AP2 σ antibodies. B and C, IF analysis in root cells with affinity-purified anti-AP2 μ and anti-AP2 σ primary antibodies and Cy3-labeled anti-rabbit secondary antibodies, respectively.

D, Indirect immunodetection of AP1/2 β 1 in the wild-type root cells using affinity-purified anti-AP1/2 β 1 primary antibodies. Antibody binding was visualized using Cy3-labeled anti-rabbit secondary antibodies (left panel), while control immunolabeling with the Cy3-labeled second antibodies in the absence of primary antibodies (-/Cy3; right panel).

E to G, IF analysis of intracellular co-localization of AP1/2 β 1 with clathrin. E, Representative images for AP1/2 β 1 and CLC1-GFP intracellular localization in the root cells. F, A scatter-plot image from (E) shows partial co-localization of AP1/2 β 1 with CLC1-GFP, quantified by the linear Pearson correlation coefficient (r_p) and the nonlinear Spearman rank correlation coefficient (r_s) indicated in the image. $r = 1.0$ means complete co-localization of two fluorescent signals. G, Average levels of r_p and r_s from five independent confocal images.

Arrows show specific bands of AP2 μ and AP2 σ (A) or AP1/2 β 1 localization at the intracellular compartments (D) or its co-localization with CLC1-GFP (E). Arrowheads show PM-associated AP2 μ and AP2 σ (B and C) or AP1/2 β 1 localization at the undefined intracellular compartments (D). Asterisks (A) denote nonspecific polypeptide bands unrelated to AP2 μ and AP2 σ that crossreact with the anti-AP2 μ and -AP2 σ antibodies. Shown are means \pm SD. Scale bars = 10 μ m (B, C, and D), 5 μ m (E).



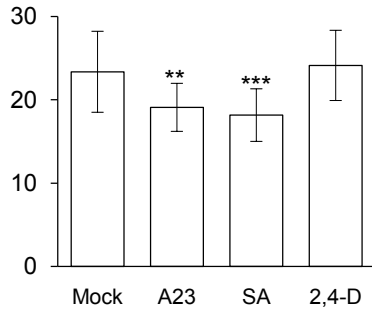
Supplemental Figure S8. Effects of High Concentrations of TyrA23 and SA on the PM Association of AP-2 Subunits.

A to R, Treatments with TyrA23 or SA for 30 min in the seedlings expressing AP2α1-GFP, or AP2μ-YFP (false-colored-green), or AP2σ-GFP.

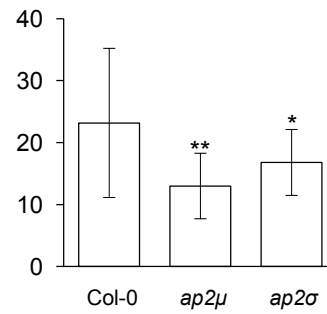
F, L, and R, The relative intensities of PM-associated GFP- or YFP-fused AP-2 subunits ($n = 128-156$ cells from 8 roots each).

Treatments with mock (DMSO), TyrA23 (A23; 60 and 90 μM), and SA (50 and 100 μM) and duration time (30 min) are indicated at the top of the panels. Arrowheads show PM-associated GFP- or YFP-fused AP-2 subunits. Shown are means \pm SD. Single, double, triple asterisks indicate $P < 0.05$, 0.001, and 0.0001, respectively (Student's t test; compared with the mock control). Scale bars = 10 μm.

A Average number of AP1/2 β 1-labeled intracellular compartments per cell



B Average number of AP1/2 β 1-labeled intracellular compartments per cell

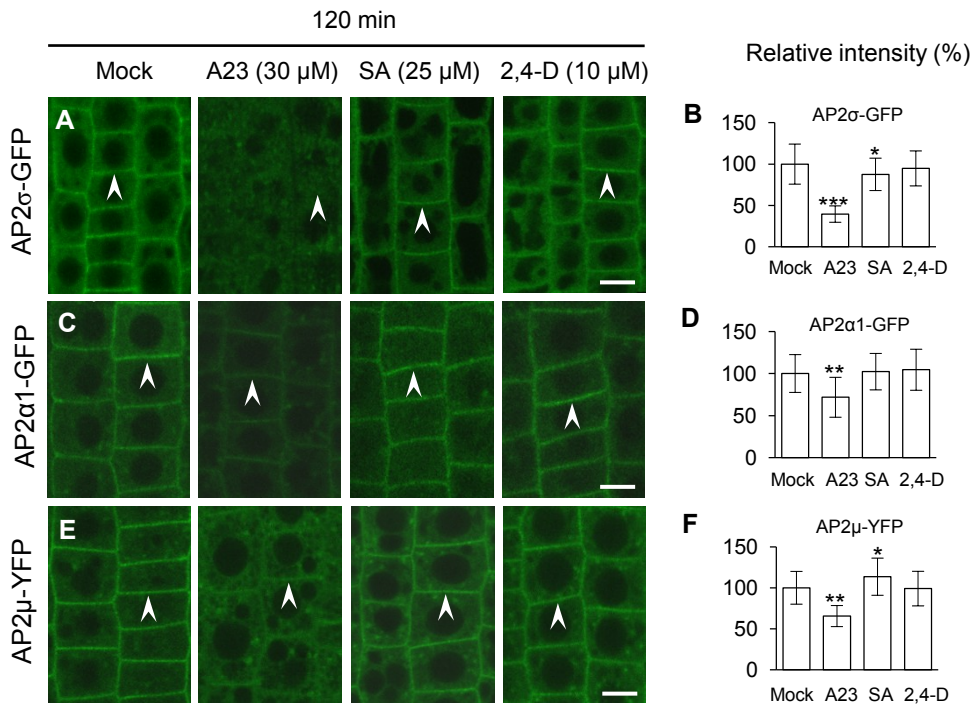


Supplemental Figure S9. Quantification Analysis of AP1/2 β 1 Intracellular Signals in Figure 4 and Figure 5.

A, The average number of AP1/2 β 1-labeled intracellular compartments (corresponding to Figure 4, I; $n = 20$ -30 cells from 3 or 4 seedlings each)

B, The average number of AP1/2 β 1-labeled intracellular compartments (corresponding to Figure 5; A and B; G and H; $n = 42$ -63 cells from 4 or 5 seedlings each).

Shown are means \pm SD. Single, double, and triple asterisks indicate $P < 0.05$, 0.01 (B) or 0.001 (A), and 0.0001, respectively (Student's t test; compared with the mock control or the wild type).

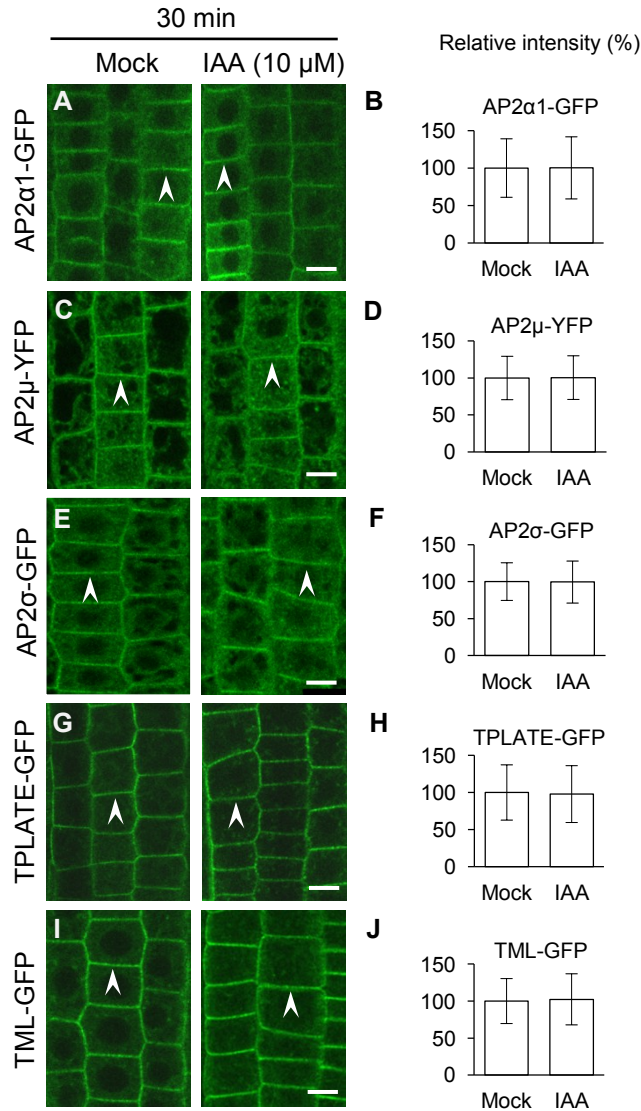


Supplemental Figure S10. Impacts of CME Effectors/Inhibitor on the PM Association of AP-2 Subunits in Extended Treatment.

A to F, Extended treatments (120 min) with CME effectors in the seedling expressing AP2 σ -GFP or AP2 α 1-GFP or AP2 μ -YFP (false-colored-green).

B, D, and F, The relative intensities of PM-associated GFP- or YFP-fused AP-2 subunits ($n = 160$ -250 cells from 8-12 roots each).

Treatments with mock (DMSO), TyrA23 (A23; 30 μ M), SA (25 μ M), and 2,4-D (10 μ M) and duration time are indicated at the top of the panel, respectively. Arrowheads show PM-associated GFP- or YFP-fused AP-2 subunits. Shown are means \pm SD. Single, double, triple asterisks indicate $P < 0.05$, 0.001, and 0.0001, respectively (Student's t test; compared with the mock control). Scale bars = 10 μ m.



Supplemental Figure S11. Exogenous IAA Effect on the PM Association of the AP-2 and TPC Subunits.

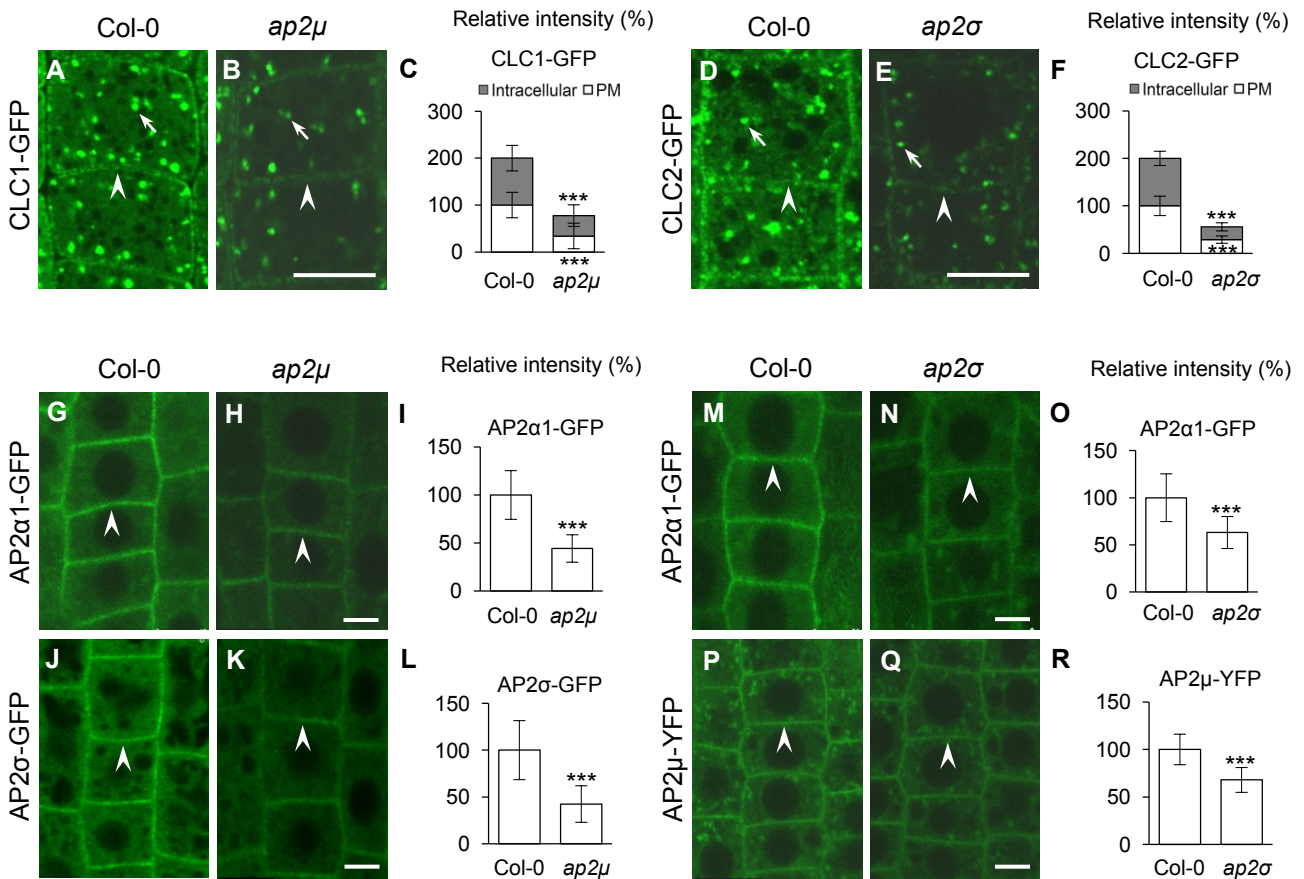
A to F, The effect of IAA treatment on the PM association of AP2 α 1-GFP (A and B), AP2 μ -YFP (C and D), and AP2 σ -GFP (E and F).

G to J, The effect of IAA treatment on the PM association of TPLATE-GFP (G and H) and TML-GFP (I and J).

B, D, and F, The relative intensities of PM-associated GFP- or YFP-fused AP-2 subunits (n = 472-817 cells from 18-20 roots each).

H and J, The relative intensities of PM-associated GFP-fused TPC subunits (n = 537-603 cells from 15 roots each).

Arrowheads show PM-associated GFP- or YFP-fused AP-2 or TPC subunits. Scale bars = 10 μ m.



Supplemental Figure S12. Membrane Association of Clathrin and AP-2 Subunits in *ap2σ* and *ap2μ*.

A to F, PM- and intracellular compartments-associated CLC1/2-GFP in the wild-type, *ap2μ*, and *ap2σ* root cells.

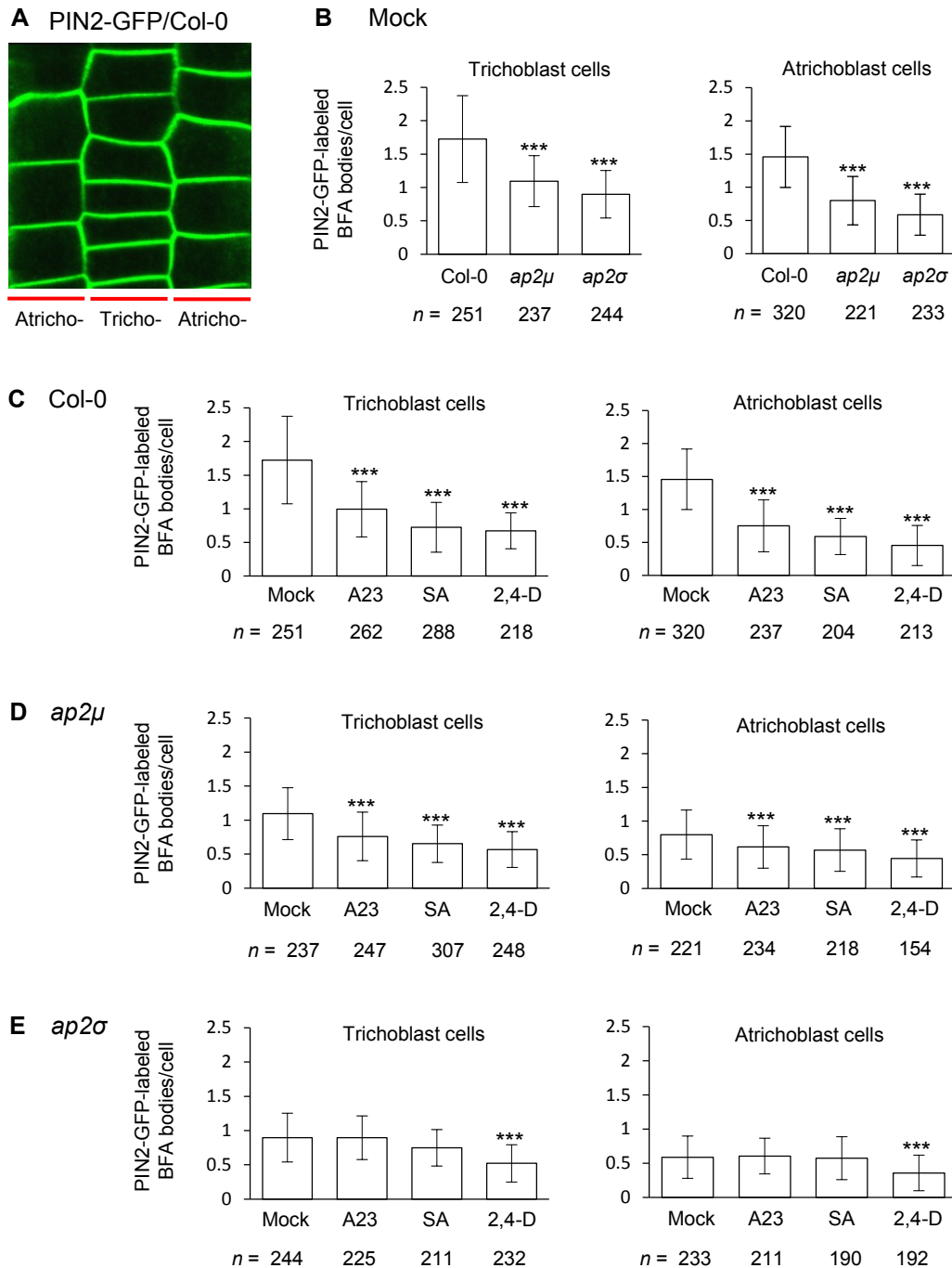
G to L, PM-associated AP2α1-GFP and AP2σ-GFP in the wild-type and *ap2μ* root cells.

M to R, PM-associated AP2α1-GFP and AP2μ-YFP in the wild-type and *ap2σ* root cells.

C and F, The relative intensities of CLC1/2-GFP at the PM and intracellular compartments ($n = 48-93$ cells from 4 roots each).

I, L, O, and R, The relative intensities of PM-associated GFP- or YFP-fused AP-2 subunits at the PM ($n = 145-265$ cells from 8 roots each; the quantitative data were summarized in Table 1).

Arrows show PM-associated GFP-fused CLC1/2 subunits, whereas arrowheads show intracellular compartments-associated CLC1/2-GFP or PM-associated fluorescently tagged AP-2 subunits. Shown are means \pm SD. Triple asterisks indicate $P < 0.0001$ (Student's t test). Scale bars = 10 μ m.



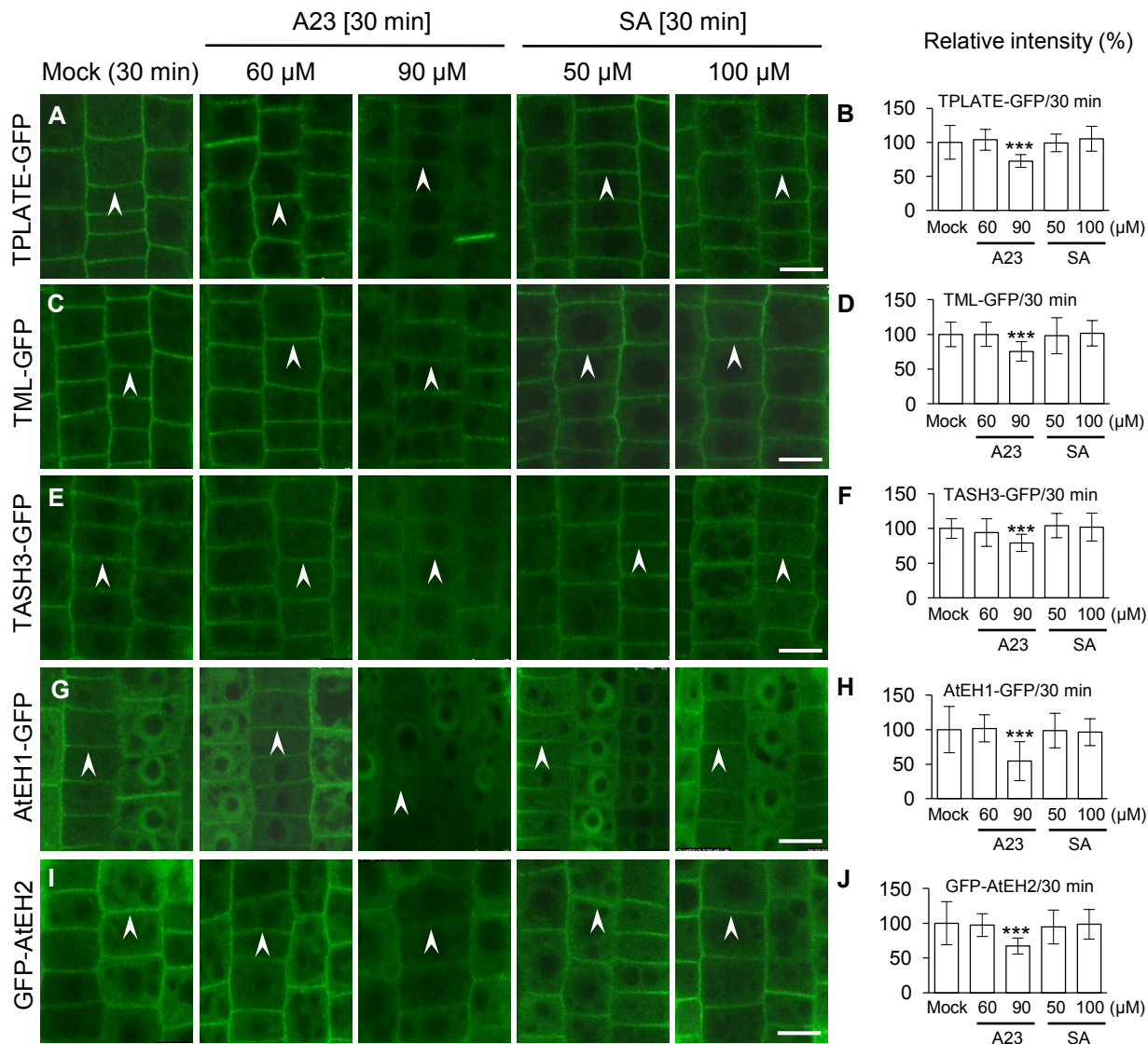
Supplemental Figure S13. Quantification Analysis of PIN2 Endocytosis in Trichoblast and Atrichoblast Cells in Figure 6.

A, A representative confocal image showing trichoblast and atrichoblast cells of the root expressing PIN2-GFP.

B, The effect of loss of AP2 μ or AP2 σ on PIN2-GFP internalization in trichoblast and atrichoblast cells treated with mock (corresponding to Fig. 6, B, H, N).

C to E, Impacts of CME effectors/inhibitor on PIN2-GFP internalization in trichoblast and atrichoblast cells of the wild type (C; corresponding to Fig. 5, B to E), *ap2μ* (D; corresponding to Fig. 5, H to K), and *ap2σ* (E; corresponding to Fig. 6, N to Q). Mock controls in (C to E) are identical with those in (B), respectively.

Shown are means \pm SD. Triple asterisks indicate $P < 0.0001$ (Student's t test; compared with the corresponding wild-type or mock control). n , the total number of examined cells from 11-15 seedlings as indicated at the bottom of graphs.



Supplemental Figure S14. Effects of High Concentrations of TyrA23 and SA on the PM Association of the TPC Subunits.

A to J, Treatments with TyrA23 or SA for 30 min in the seedlings expressing GFP-fused TPC subunits.

B, D, F, H, and J, The relative intensities of PM-associated GFP-fused TPC subunits ($n = 48-120$ cells from 4 roots each).

Treatments with mock (DMSO), TyrA23 (A23; 60 and 90 μM), and SA (50 and 100 μM) and duration time are indicated at the top of the panels. Arrowheads show PM-associated GFP-fused TPC subunits. Shown are means \pm SD. Triple asterisks indicate $P < 0.0001$, respectively (Student's t test; compared with the mock control). Scale bars = 10 μm .